



Characteristics of Condenser-excited Single-phase Induction Motor

著者	Ishizaki Takemitsu, Fujii Tomoo, Ishikawa Sadao, Hirasa Takao
引用	Bulletin of University of Osaka Prefecture. Series A, Engineering and natural sciences. 1970, 19(1), p.75-86
URL	http://doi.org/10.24729/00008854

Characteristics of Condenser-excited Single-phase Induction Motor

Takemitsu ISHIZAKI*, Tomoo FUJII*, Sadao ISHIKAWA*
and Takao HIRASA*

(Received June 15, 1970)

This paper deals with the theoretical equation to estimate the characteristics of the condenser-excited single-phase induction motor and its experimental characteristics. Its characteristics at rated frequency 60 (Hz) varied with size of exciting condenser. Optimum operation can be obtained at minimized negative-phase sequence current. In optimum operation of sample motor, no-load current decrease by 60 percent, full load efficiency increase 10 percent, and pulsating torque of double stator frequency which introduce vibration and noise to motor decrease 30~70 percent compared with the ordinary single-phase induction motor

The optimum value C_{op} of exciting condenser, in which optimum characteristics can be obtained, vary with frequency f and magnetizing inductance l_{ϕ} . Relation among them is simply represented as

$$C_{op}f^2l_{\phi}=\text{constant}$$

Tests are carried out over frequency range from 30 (Hz) to 70 (Hz) in order to verify this relation. The speed of condenser-excited motor can be controlled more smoothly, silently, and efficiently than ordinary single-phase induction motor. Use of exciting condenser for single-phase induction motor in the speed control systems is suggested in this paper.

1. Introduction

The single-phase induction motors are very widely used in appliances, in business, and in industry. They find interesting applications in automatic control devices of various kinds.

In previous papers^{1,2)} control characteristics of condenser-excited single-phase induction motor driven by thyristor inverter were reported, and its controlling characteristics indicated such excellent results that were never obtained by the ordinary single-phase induction motor. In this case, the wave form of the source voltage which is supplied to the motor by inverter is a very distorted one. Very little work has been done to estimate the control characteristics of condenser-excited motor driven by the ordinary sinusoidal wave source.

This paper deals with the theoretical equation to estimate the characteristics of the condenser-excited single-phase induction motor and its experimental characteristics driven by sinusoidal wave source over frequency range from 30 (Hz) to 70 (Hz).

* Department of Electrical Engineering, College of Engineering.

2. Condenser-excited Single-phase Induction Motor

2-1. Principle Condenser-excited motor resembles condenser motor except for connection of the stator windings. They are connected as shown in Fig. 1. The main winding M is connected to a single-phase source and the auxiliary winding A is short circuited through a condenser C . When the motor is in running condition, a voltage E_a is generated in the auxiliary winding by the rotation of rotor in the field which is energized from the voltage V_m . The auxiliary winding current I_a in the condenser C , is out of phase with the current I_m in the main winding M . Both currents are equivalent to two-phase exciting currents and can generate the rotating field in the motor. Such a motor can be called "condenser-excited single-phase induction motor⁸⁾" because of the condenser C serves for the excitation of the motor. This motor has no starting torque, but if started by auxiliary means, it will continue to run efficiently and noiselessly.

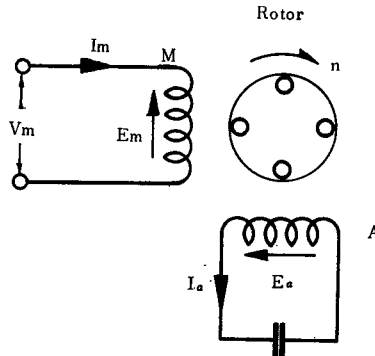


Fig. 1 Connection of Condenser-excited motor.

2-2. Calculation of characteristics The stator windings of the motor indicated in Fig. 1, are in electrical space quadrature each other and may have unequal turns. The voltage equations in stator circuits can be written as follows

$$\left. \begin{aligned} (r_m + jx_m)I_m + E_m &= V_m \\ \{r_a + j(x_a - x_c)\}I_a + E_a &= 0 \end{aligned} \right\} \quad (1)$$

where r_m , r_a and x_m , x_a are the effective resistances and leakage reactances of the windings M , A , respectively; $x_c = 1/2\pi fC$ is a capacitive reactance of C ; and E_m is the counter emf generated in the winding M . Method of symmetrical co-ordinates is applied to eq. (1). Then the positive- and negative-phase sequence components of the stator phase currents are

$$I_P = \frac{1}{2}(I_m - jaI_a), \quad I_N = \frac{1}{2}(I_m + jaI_a) \quad (2)$$

where $a(=N_a/N_m)$ is the effective turn ratio. Note that $a \times I_a$ is the current in winding A referred to winding M . The positive- and negative-phase sequence components of the applied voltage and the induced emfs are

$$V_P = V_N = \frac{1}{2} V_m \quad (3)$$

$$E_P = \frac{1}{2}(E_m - j\frac{1}{a}E_a), \quad E_N = \frac{1}{2}(E_m + j\frac{1}{a}E_a) \quad (4)$$

The positive- and negative-phase sequence components of the sum of the external impedance and the leakage impedance of the stator phase windings are

$$\left. \begin{aligned} Z_P &= \frac{1}{2} \left[r_m - \frac{r_a}{a^2} + j \left(x_m - \frac{x_a}{a^2} + \frac{x_c}{a^2} \right) \right] \\ Z_N &= \frac{1}{2} \left[r_m + \frac{r_a}{a^2} + j \left(x_m + \frac{x_a}{a^2} - \frac{x_c}{a^2} \right) \right] \end{aligned} \right\} \quad (5)$$

When the rotor is running at a slip s , the positive- and negative-phase sequence components of the rotor and magnetizing impedance Z_P and Z_N as viewed from winding M are given by the equivalent circuits shown in Fig. 2. Therefore Z_P and Z_N can be written as follows

$$\begin{aligned} Z_P &= \frac{E_P}{I_P} = \frac{1}{\frac{1}{jx_\phi} + \frac{1}{r_2/s + jx_2}} = \frac{\left(\frac{r_2}{s} \right) x_\phi^2 + j \left[\left(\frac{r_2}{s} \right)^2 x_\phi + x_2 x_\phi (x_2 + x_\phi) \right]}{\left(\frac{r_2}{s} \right)^2 + (x_2 + x_\phi)^2} \\ &\equiv R_P + jX_P \end{aligned} \quad (6)$$

$$\begin{aligned} Z_N &= \frac{E_N}{I_N} = \frac{1}{\frac{1}{jx_\phi} + \frac{1}{r_2/(2-s) + jx_2}} = \frac{\left(\frac{r_2}{2-s} \right) x_\phi^2 + j \left[\left(\frac{r_2}{2-s} \right)^2 x_\phi + x_2 x_\phi (x_2 + x_\phi) \right]}{\left(\frac{r_2}{2-s} \right)^2 + (x_2 + x_\phi)^2} \\ &\equiv R_N + jX_N \end{aligned} \quad (7)$$

Equations (1) to (7) can be solved for the positive- and negative-phase sequence

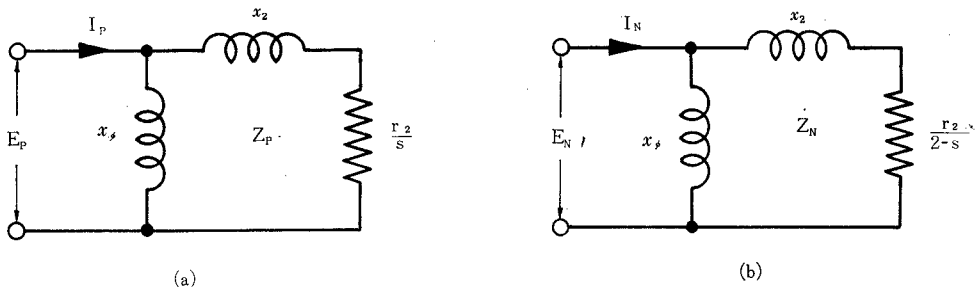


Fig. 2 Equivalent circuits representing (a) the positive and (b) negative-phase sequence components of the rotor and magnetizing impedances as viewed from the main winding.

currents, giving

$$I_P = \frac{z_N - z_P + Z_N}{Z_P Z_N + z_N(Z_P + Z_N) + z_N^2 - z_P^2} \cdot \frac{V_m}{2} \quad (8)$$

$$I_N = \frac{z_N - z_P + Z_P}{Z_P Z_N + z_N(Z_P + Z_N) + z_N^2 - z_P^2} \cdot \frac{V_m}{2} \quad (9)$$

Considering that x_C is a variable and rearranging these equations,

$$I_P = \frac{(r_a + a^2 R_N) + j(x_a + a^2 X_N) - jx_C}{B_1 + jB_2 + (D_1 + jD_2)x_C} \cdot V_m \quad (10)$$

$$I_N = \frac{(r_a + a^2 R_P) + j(x_a + a^2 X_P) - jx_C}{B_1 + jB_2 + (D_1 + jD_2)x_C} \cdot V_m \quad (11)$$

where

$$\left. \begin{aligned} B_1 &= \{2a^2(R_P R_N - X_P X_N) + (a^2 r_m + r_a)(R_P + R_N) \\ &\quad - (a^2 x_m + x_a)(X_P + X_N) + 2(r_m r_a - x_m x_a)\} \\ B_2 &= \{2a^2(R_P X_N + R_N X_P) + (a^2 r_m + r_a)(X_P + X_N) \\ &\quad + (a^2 x_m + x_a)(R_P + R_N) + 2(x_m r_a + x_a r_m)\} \\ D_1 &= X_P + X_N + 2x_m \\ D_2 &= -(R_P + R_N + 2r_m) \end{aligned} \right\} \quad (12)$$

It can easily be seen from eqs. (10) and (11) that locus of currents are circles. Therefore circle diagram given by eqs. (10) and (11) is immediately applicable to the study of motor.

From eqs. (2), the stator phasor currents can be written,

$$\left. \begin{aligned} I_m &= I_P + I_N \\ I_a &= j(I_P - I_N)/a \end{aligned} \right\} \quad (13)$$

The torque in synchronous watts developed by the motor is

$$T = 2(I_P^2 R_P - I_N^2 R_N) \quad (W) \quad (14)$$

In addition to the torque T , double-stator-frequency torque pulsation is produced in the single-phase induction motor. This pulsating torque is unavoidable in a single-phase motor because of the pulsation in instantaneous power input inherent in a single-phase circuit. It tends to make the motor noisier than a poly-phase motor. Its peak value T_V^{5-7} is represented by

$$T_V = 2|I_P| \times |I_N| \times |Z_P - Z_N| \quad (W) \quad (15)$$

Let β be the ratio of T_V to T , then β may be called "pulsating torque factor".

$$\beta = T_V / T \times 100 \quad (\%) \quad (16)$$

Input and output power and efficiency of the motor can be written as follows

$$\left. \begin{aligned} P_i &= V_m I_m \cos \theta & (W) \\ P_o &= (1-s)T & (W) \\ \eta &= \frac{P_o}{P_i} \times 100 & (\%) \end{aligned} \right\} \quad (17)$$

where θ is phase difference between V_m and I_m .

3. Experimental results

Motor employed for the tests is a condenser start single-phase induction motor. Its specifications and circuit constants are indicated in Table 1. A torque-meter serves as the motor load.

Table 1 Specifications and circuit constants of condenser start single-phase induction motor

Specifications			
Voltage	100 (V)	output	200 (W)
frequency	60/50 (Hz)	speed	1730/1440 (rpm)
No. of poles	4	Starting condenser	150 (μ F)
Circuit constants in (Ω)			
rotor referred to main winding		$r_2=2.84$	$x_2 = 1.96$
magnetizing reactance referred to main winding			$x_\phi = 59.72$
main winding		$r_m=1.97$	$x_m = 1.96$
auxiliary winding		$r_a=9.75$	$x_a = 4.91$
Effective turns ratio	$N_a/N_m=a=1.59$		

Note; Value of reactances obtained on the frequency 60 (Hz)

3-1.No-load tests The slip of motor at no-load running is nearly equals to 0.005. The circle diagrams of the positive- and negative-phase sequence currents I_P , I_N at slip $s=0.005$, frequency $f=60(\text{Hz})$ and $V_m=100(\text{V})$, are shown in Fig. 3.

In this figure $I_P(15)$ and $I_N(15)$, $I_m(15)$ and $I_a(15)$ indicate the positive- and negative-phase sequence currents, main and auxiliary winding currents at $C=15(\mu\text{F})$; $I_P(0)$, $I_N(0)$ and $I_m(0)$ indicate the currents of ordinary single-phase motor which has no exciting condenser i.e. $C=0$. Phase difference angle between $I_m(15)$ and $I_a(15)$ equals to 72 deg.. After this, number in the parentheses of current, input P_i , torque pulsation factor β etc. indicate the capacity of exciting condenser in μF .

The no-load running tests are carried out over the frequency range from 30(Hz) to 70 (Hz). The experimental characteristics of I_m , I_a , P_i and power factor $\cos \theta$ vs. C at $V_m=100(\text{V})$, $f=60(\text{Hz})$, $s=0.005$ are shown in Fig. 4. As compared with values of ordinary single-phase induction motor, $I_m/I_m(0)$, $P_i/P_i(0)$, $\beta/\beta(0)$ vs. C characteristics are shown in Fig. 5. In this figure, $I_m/I_m(0)$ and $P_i/P_i(0)$ are indicated experimental results, $\beta/\beta(0)$ are indicated the theoretical values because of the pulsating torques were not measured in these tests. This pulsating torque tend to make the motor noisier than a poly-phase motor, can be minimized by use of the exciting condenser for the motor. Optimum no-load running can be obtained at minimum input and minimum pulsating torque.

From Fig. 5, it is readily seen that (1) no-load input i.e. no-load loss and pulsating torque factor are minimum at $C \approx 15(\mu\text{F})$, i.e. optimum no-load running is obtained at this point; (2) in optimum operation, no-load current, loss and pulsating

torque factor decrease by 40, 33 and 72 percent, respectively, compared with ordinary single-phase motor operation; (3) I_m is minimum at $C \approx 30(\mu F)$, the minimized current I_{min} decrease 73 percent.

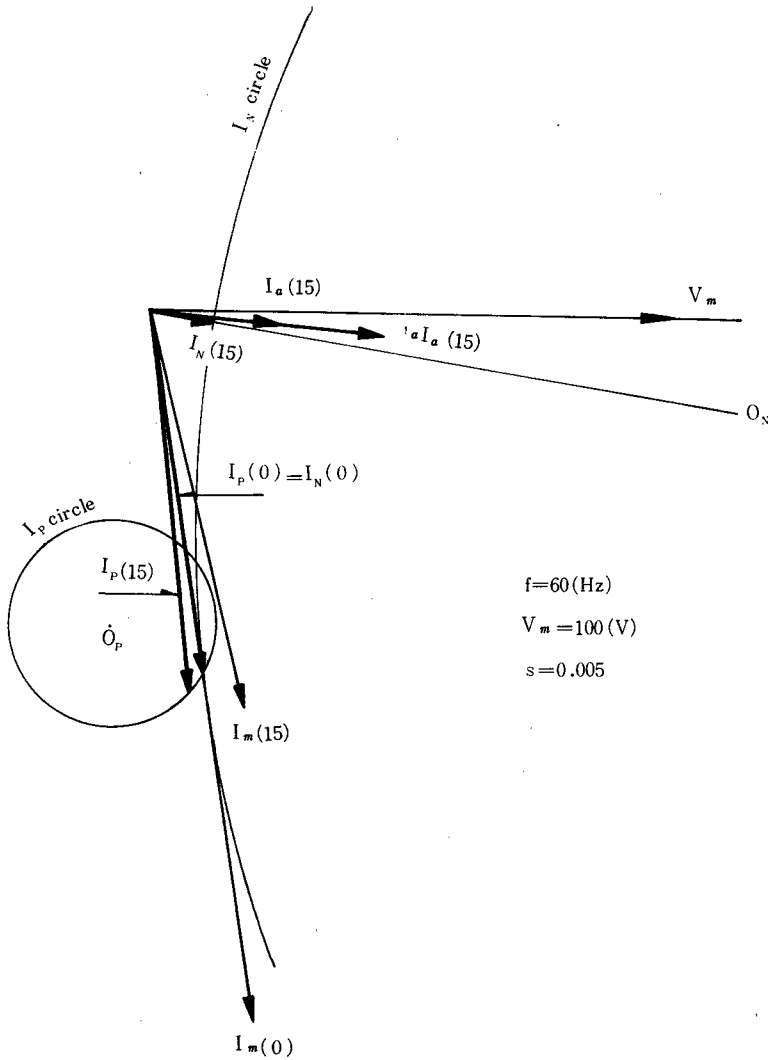
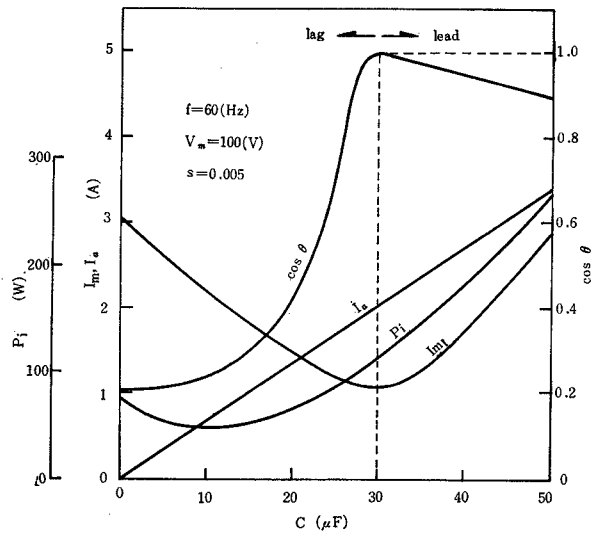
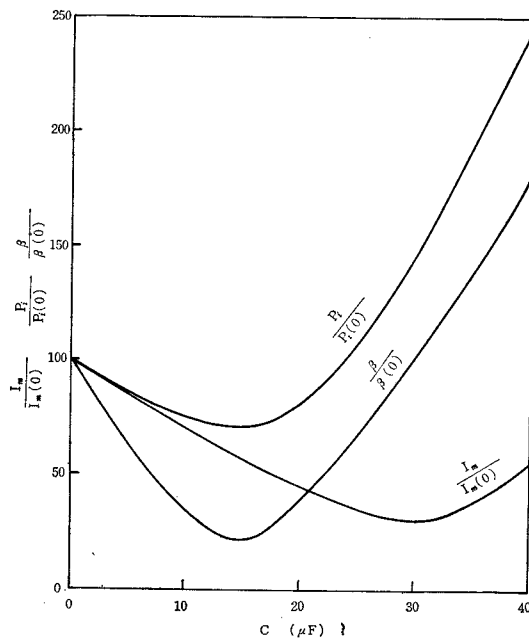


Fig. 3 Circle diagrams of the positive and negative-phase sequence currents.



I_m : main winding current I_a : auxiliary winding current
 P_i : input power $\cos \theta$: power factor

Fig. 4 No-load characteristics I_m , I_a , P_i and $\cos \theta$ vs. C .



β : torque pulsation factor
 $\beta(0)$: value of β at $C=0$

Fig. 5 No-load characteristics $\frac{I_m}{I_m(0)}$, $\frac{P_i}{P_i(0)}$ and $\frac{\beta}{\beta(0)}$ vs. C .

3-2. Simplified equation to determine optimum value of condenser The optimum value of condenser in which the negative-phase sequence current I_N is minimized, is determined by the condition the $dI_N/dC=0$. This calculation gives trouble. For simplicity, r_m , x_m , r_a , x_a and x_2 are neglected compare with r_2/s , because of $s \simeq 0$ at no-load running of the motor. Optimum condenser C_{0P} is given

$$C_{0P} \simeq \frac{1}{a^2 \omega x_\phi} = \frac{1}{4\pi^2 a^2 f^2 l_\phi} \quad (\mu F) \quad (18)$$

where $l_\phi = x_\phi / 2\pi f$ is a magnetizing inductance.

The value of condenser at minimum main winding current denoted as C_{mi}

$$C_{mi} \simeq \frac{1}{2\pi^2 a^2 f^2 l_\phi} = 2C_{0P} \quad (\mu F) \quad (19)$$

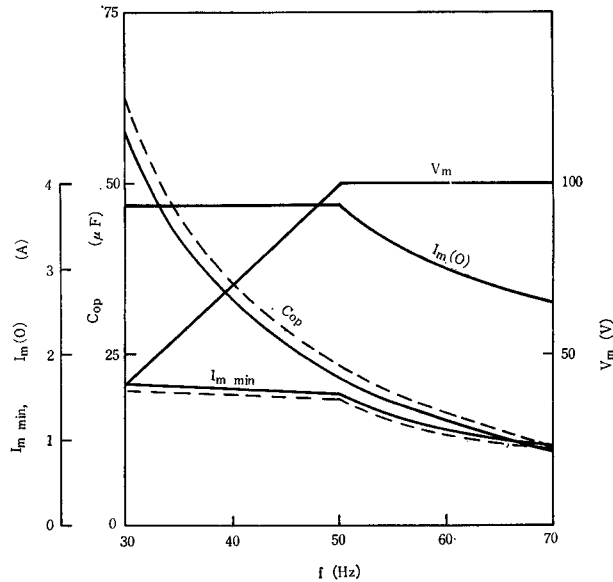


Fig. 6 Frequency characteristics at no-load C_{0P} and $I_{m \min}$ vs. f .

Eq. (19) is verified by no-load test as shown in Fig. 4, 5.

Frequency characteristics of C_{0P} and $I_{m \min}$ are shown in Fig. 6. In this test, the supplied voltage V_m of the motor are regulated to be nearly proportional to the frequency of power source for maintained the constant field flux i.e. constant exciting current $I_m(0)$ at $f < 50(\text{Hz})$, and equals to the rated voltage $100(\text{V})$ at $f \geq 50(\text{Hz})$ as shown in Fig. 6. Experimental curves for C_{0P} and $I_{m \min}$ are indicated by the solid lines, and the theoretical values by the dotted lines. Fairly agreement between the experimental and theoretical curves is seen from Fig. 6. No-load tests verified eqs. (18) and (19).

3-3. Load tests The load tests at rated speed i.e. rated slip are carried out over the frequency range from $30(\text{Hz})$ to $70(\text{Hz})$. The experimental characteristics

of I_m , I_a , output P_o and efficiency η vs. C at $V_m=100(V)$, $f=50(Hz)$, $S \simeq 0.04$ i.e. speed 1440 (*rpm*) are shown in Fig. 7. It is seen that optimum and minimum current running can be obtained at $C \simeq 20 (\mu F)$ and $C \simeq 40 (\mu F)$, respectively. Fig. 8 shows characteristics of η and I_m at $V_m=100(V)$, $f=50(Hz)$ $n=1440$ (*rpm*), where $\eta(20)$ and $I_m(20)$ represent values of η and I_m at optimum running; $\eta(40)$, $I_m(40)$ and $\eta(0)$, $I_m(0)$ represent the values at minimum current and ordinary single phase

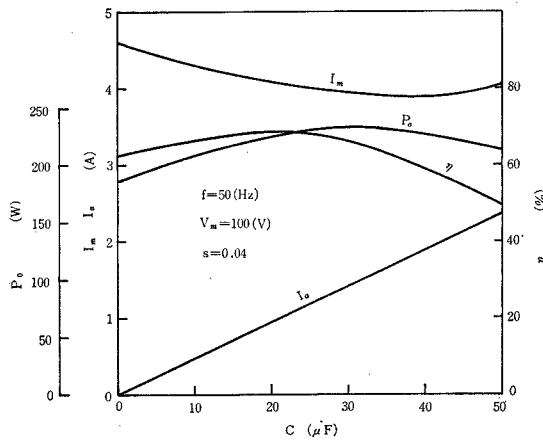


Fig. 7 Load characteristics I_m , I_a , P_o and η vs. C .

running, respectively. It can be seen, from Fig. 8, that $\eta(20)$ is larger than $\eta(0)$, $\eta(40)$ is smaller than $\eta(0)$ at power range from no-load to 25 percent over load.

$I_m/I_m(0)$, $\eta/\eta(0)$, $P_o/P_o(0)$, $\beta/\beta(0)$ vs. C characteristics are shown in Fig. 9, for compared the values of ordinary single-phase motor with ones of condenser-excited

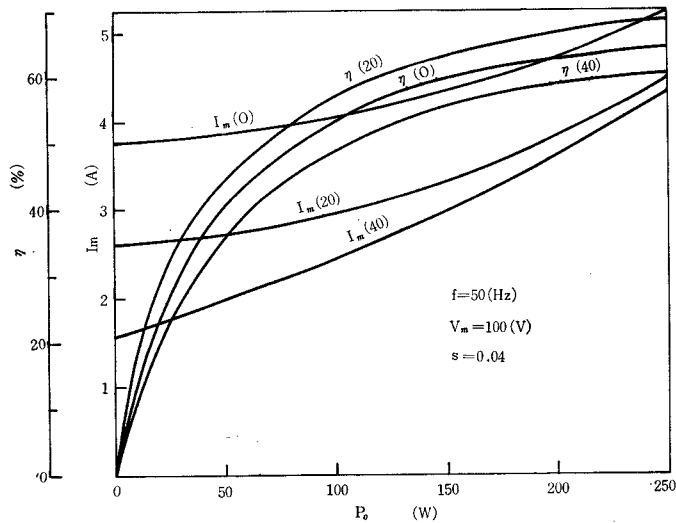


Fig. 8 Load characteristics I_m and η vs. P_o .

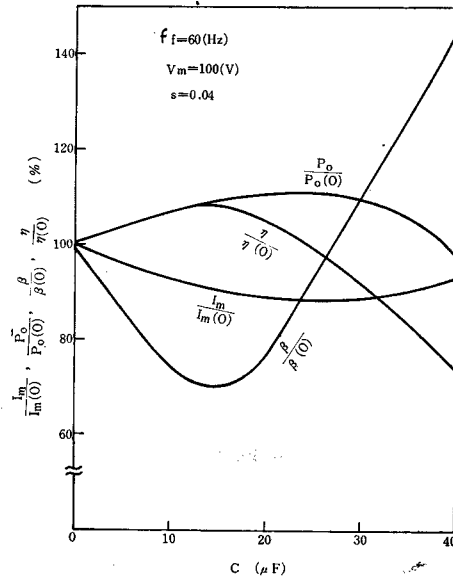


Fig. 9 Load characteristics $\frac{I_m}{I_m(0)}$, $\frac{P_0}{P_0(0)}$, $\frac{\beta}{\beta(0)}$ and $\frac{\eta}{\eta(0)}$ vs. C .

motor at rated speed 1730(rpm) i.e. $f=60(Hz)$. In that figure, $\beta/\beta(0)$ are indicated theoretical values, and others are experimental ones. From Fig. 9, it is seen that current $I_m(15)$ and pulsating torque factor $\beta(15)$ at optimum full load running decreased by 10 and 30 percent than $I(0)$ and $\eta(0)$ respectively ; $P_0(15)$ and $\eta(15)$ increase 10 and 12 percent than $P_0(0)$ and $\eta(0)$.

Frequency characteristics of full load running are shown in Fig. 10. In these

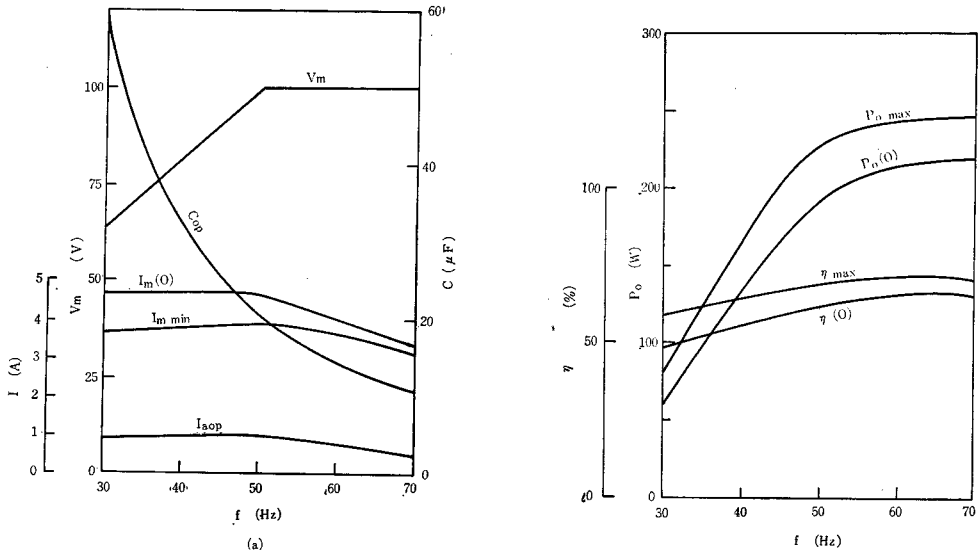


Fig. 10 Frequency characteristics at $s=0.04$ (a) C_{OP} , $I_{m\min}$ and I_{aOP} vs. f , (b) $P_{0\max}$, $P_0(0)$, η_{\max} and $\eta(0)$ vs. f .

tests as well as no-load frequency tests, the supplied voltage V_m of the motor are regulated to be nearly proportional to the frequency of power source at $f < 50$ (Hz) and equal to the rated voltage 100 (V) at $f \geq 50$ (Hz) and the slip is kept the rated value 0.04. C_{0P} , $I_m(0)$, I_{mmin} and I_{a0P} vs. f characteristics are shown in Fig. 10(a), where I_{a0P} indicate the auxiliary winding current at optimum running. $P_o max$, $P_o(0)$, η_{max} and $\eta(0)$ are shown in Fig. 10(b), it is readily seen that high output power and high efficiency at small main input current of motor can be obtained by the use of exciting condenser. Full load tests as well as no-load tests verified the following relation

$$C_{0P} f^2 l_\phi \simeq k$$

Discussion of frequency characteristics and torque pulsation are omitted in this paper, it will be reported later publication.

4. Conclusion

The running characteristics of condenser-excited single-phase induction motor vary with exciting condenser which is connect to auxiliary winding. Optimum running motor can be obtained at minimized negative-phase sequence current. The optimum value C_{0P} of exciting condenser, in which optimum characteristics can be obtained, is represented by eq. (18) i.e.

$$C_{0P} \simeq k / (f^2 l_\phi)$$

The theoretical calculations and experimental tests carried out over frequency ranges from 30(Hz) to 70(Hz), verified this relation.

In optimum no-load running of the sample motor at rated frequency, source current, loss and pulsation torque factor decrease by 40, 33 and 72 percent, respectively, as compared with values of ordinary single-phase operation in which motor has no exciting condenser.

In optimum full-load running at rated frequency, it is shown that source current and pulsating torque factor decrease by 10 and 30 percent; output power and efficiency are increased by 10 and 12 percent as compared with values of ordinary single-phase operation.

The speed of condenser-excited motor can be controlled more smoothly, silently and efficiently than ordinary single-phase motor. Use of exciting condenser for single-phase induction motor in the speed control systems is suggested in this paper.

References

- 1) S. Ishikawa, A. Ichiriki, M. Okita and T. Ishizaki, Lecture 2a-18 in Annual Meeting of Kansai Branch of I.E.E. of Japan, (November 1967).
- 2) K. Taniguchi, T. Fujii and T. Ishizaki, Lecture 3-14 in Annual Meeting of Kansai Branch of E.I.E. of Japan, (November 1968).

- 3) T. Hasumi. OHM, **37**, 13 (1950).
- 4) S. Miyairi. J.I.E.E. of Japan, **74**, 31 (1954).
- 5) J. Kibe, S. Mito and K. Kamimura, J.I.E.E. of Japan, **82**, 190 (1962).
- 6) A. Morishita, J. Kataoka, H. Watanabe and S. Okuda, Lecture 559 in Annual Meeting of I.E.E. of Japan, (March 1969).
- 7) T. Yokozuka, E. Baba, M. Ohki and Y. Kozu, Lecture 518 in Annual Meeting of I.E.E. of Japan, (April 1970).